Research Article

Bacterial Fluorescence-Based Biosensor for Detecting Propionate in Culture Media for Diagnostic Applications

Biomarker Insights
Volume 21: 1–15

DOI: 10.1177/11772719261455896
journals.sagepub.com/home/bmi

Salvador Fabela[1,*], Camilo P. Martínez-Reyes[1,*], Rene Arredondo-Hernandez[2,*], Gonzalo Castillo-Rojas[1], Patricia Orduña[2], Enrique O. Graue-Hernández[3], and Yolanda López-Vidal[1]

Abstract

Background: Engineering bacteria for disease diagnosis and treatment is an emerging area of medical research that involves assessing short-lived molecules in complex, dynamic environments. Detecting metabolites *in situ* offers significant opportunities for identifying responsive cellular populations. Among suitable targets for this technology are short-chain fatty acids, such as propionate, that play crucial roles in human health and disease. **Objective:** To develop a bacterial fluorescence-based biosensor capable of detecting propionate levels at the millimolar scale in low-volume samples across different culture media and optimize its application protocol. **Methods:** Using *Escherichia coli* strain BL21(DE3) transformed with the pPro24-GFP plasmid, which contains the green fluorescent protein (*GFP*) gene under the control of a propionate-inducible promoter, we achieved reliable propionate detection with a threshold of 10 mM in a small volume (750 μL). **Results:** The fluorescence-based biosensor functioned in both Luria–Bertani and Dulbecco's modified Eagle media, producing fluorescence intensities of 3863 ± 957 arbitrary units. Validation using a portable Qubit® 3.0 fluorometer yielded a receiver operating characteristic curve with a Cohen's kappa of 0.716, indicating substantial agreement. Proof-of-concept experiments using flow cytometry and mock fecal samples (healthy feces + 100 mM propionate) successfully detected the elevated propionate levels. **Conclusion:** This cost-effective, easy-to-use protocol provides a proof-of-concept for propionate detection in biological samples, with potential future applications in clinical diagnostics, particularly for gastrointestinal disorders in which propionate serves as a biomarker, where it could be used to monitor disease progression and therapeutic interventions.

Keywords

microbial fluorescence-based biosensor, propionate detection, diagnostics, metabolic activity, low-volume samples, short-chain fatty acids, inflammatory bowel disease

Received: 30 January 2026; Revised: 6 May 2026; Accepted: 13 May 2026

[1]Programa de Inmunología Molecular Microbiana, Departamento de Microbiología y Parasitología, Facultad de Medicina, Universidad Nacional Autónoma de México, Ciudad de México, Mexico
[2]Laboratorio de Microbioma, División de Investigación, Facultad de Medicina, Universidad Nacional Autónoma de México, Ciudad de México, Mexico
[3]Cornea and Refractive Surgery Department, Institute of Ophthalmology, Fundación de Asistencia Privada Conde de Valenciana, Mexico City, Mexico

*These authors contributed equally.

Corresponding author:
Yolanda López-Vidal, Programa de Inmunología Molecular Microbiana, Edificio H, 4° piso, Departamento de Microbiología y Parasitología, Facultad de Medicina, Universidad Nacional Autónoma de México-Ciudad Universitaria, Del. Coyoacán, CP 04510, Ciudad de México, Mexico.
Email: lvidal@unam.mx

Introduction

Short-chain fatty acids (SCFAs) are small monocarboxylic organic acids containing up to six carbon atoms. In humans, SCFAs are primarily produced by bacteria in the large intestine through the anaerobic fermentation of indigestible polysaccharides, such as dietary fiber and resistant starch.[1,2] The three predominant SCFAs—acetate (C_2), propionate (C_3), and butyrate (C_4)—are typically found at a molar ratio of 60:20:20 in the human intestine.[3,4] Quantification of SCFAs in biological samples relies on mass spectrometry, limiting the scalability of metabolomic data from translational research to clinical application.

While butyrate's beneficial effects on human health have been extensively documented,[1,5-7] the mechanisms by which bacteria sense butyrate remain incompletely understood, despite reports of quorum responses of *Escherichia coli*.[8-10] In contrast, their mechanisms for detecting acetate and propionate have been fully elucidated and are amenable to bioengineering. First characterized in *Pseudomonas fluorescens* and present in *Vibrio cholerae* and *Pseudomonas entomophila*, the acetate-sensing system operates through the CrbS/R two-component signal transduction pathway. This system regulates acetate utilization when the hybrid histidine kinase CrbS activates the cognate response regulator CrbR, which then induces the transcription of *acs* (acetyl-CoA synthetase) and *actP* (acetate/solute symporter).[11-13]

The propionate-sensing mechanism has also been comprehensively described in *Salmonella enterica* serovar Typhimurium LT2. In this bacterium, the *prpRBCDE* operon encodes a transcriptional activator (PrpR) and four enzymes involved in the 2-methylcitrate cycle that mediates growth on propionate as the sole carbon source. Propionate, a weak acid able to permeate the outer cell membrane, is metabolized through the 2-methylcitrate cycle by enzymes expressed from the chromosome-encoded *prpEC* operon. PrpR binds to an enhancer-like element located upstream (5′) of the *prpBCDE* promoter and contacts the σ^{54}-dependent RNA polymerase by forming a DNA loop, thereby activating the *prpBCDE* operon.[14-18]

Lee and Keasling[19] successfully cloned the genes involved in bacterial propionate detection into the plasmid pPro24, aiming to develop an inducible expression system based on an alternative inducer to isopropyl β-D-1-thiogalactopyranoside (IPTG) or arabinose. While the arabinose-inducible promoter (P_{BAD}) is weaker than the IPTG-inducible promoter (P_{tac}) and IPTG can diffuse freely through membranes without transporter assistance, IPTG is non-metabolizable, expensive, and relatively toxic.[19] In contrast, the pPro24 propionate-based system offers a more economical and physiologically relevant alternative. One recent study highlighted an important advantage of pPro24: its high specificity for propionate.[20] It showed no significant induction in response to other SCFAs, such as acetate or butyrate, indicating minimal cross-reactivity with structurally similar metabolites. It also showed high sensitivity at biologically relevant propionate concentrations, with a dose–response to propionate reported up to 30–40 mM in laboratory media. Notably, the *E. coli* strain BL21(DE3) harbors a homologous *prpBCDE* operon on its chromosome, making it a suitable host for the pPro24 system. Altogether, these properties make pPro24 an attractive candidate biosensor for propionate detection in biological samples.

Although the pPro24 system was originally designed and characterized as a propionate-inducible expression system under laboratory conditions, its potential utility as a propionate biosensor in complex biological samples has not been explored. Previous studies have focused on using pPro24 to evaluate gene expression. For instance, Lee and Keasling[19] characterized the pPro24 system as an IPTG-free inducible expression tool in standard media, and Serebrinsky et al[21] established dose-dependent kinetics of green fluorescent protein (GFP) in laboratory media conditions. However, these studies did not extend the pPro24 system to clinically relevant samples. To our knowledge, this study is the first to apply the pPro24 system as a quantitative propionate-detection tool in complex biological matrices using small volumes of culture media and human fecal samples. This study primarily aimed to optimize and validate the pPro24 system for this purpose, thereby providing an economical and physiologically relevant alternative to gas chromatography–mass spectrometry (GC-MS) and high-performance liquid chromatography (HPLC) based SCFA analysis.

Propionate in Health and Disease

Propionate has several beneficial effects on human health, including ameliorating colitis and vascular calcification, reducing pro-inflammatory markers and cholesterol levels, improving insulin resistance, and regulating appetite.[22-27] These effects highlight the importance of propionate as a metabolic regulator and therapeutic target.

In healthy individuals, basal propionate levels typically range from 10–30 mM, reflecting its production under homeostatic conditions.[28] However, increasing evidence suggests that excessive propionate levels may also be associated with disease states. A systematic review examining SCFA profiles in fecal samples from patients with irritable bowel syndrome (IBS) revealed distinct patterns across disease subtypes: patients with IBS and constipation (IBS-C) showed decreased propionate levels (9.7 ± 2.1 mM), whereas those with IBS and diarrhea (IBS-D) showed significantly elevated propionate levels, surpassing 100 mM, compared with healthy individuals.[29] Furthermore, the pathogenic *E. coli* strain ZvL2, isolated

from a patient with Crohn's disease, exhibited enhanced virulence when cultured in a propionate-containing medium, with propionate inducing expression of genes associated with macrophage colonization.[30]

In oral health, patients with periodontal disease often exhibit elevated salivary propionate levels, which correlate positively with bacterial load.[31] Epidemiological studies have identified associations between periodontal disease and increased risk of Alzheimer's disease,[32,33] and propionate has been proposed as one potential microbial metabolite that may contribute to neurotoxicity and disruption of the urea cycle.[34,35] However, the available evidence is associative rather than causal.

Study Rationale and Objectives

Given the growing body of evidence linking elevated propionate levels to multiple disease states, there is a clear need for accessible, reliable methods of measuring propionate levels in biological samples. Although current analytical methods, such as GC-MS and HPLC, are accurate, they require expensive equipment, specialized training, and substantial sample volumes.

Therefore, this study aimed to develop and optimize a bacterial biosensor capable of detecting millimolar concentrations of propionate in various culture media using a simple, affordable, and accessible methodology. It evaluates the biosensor's performance under different growth conditions, validates its use with low-volume samples suitable for clinical diagnostics, and demonstrates proof-of-concept detection of propionate in complex biological matrices, including fecal samples.

Materials and Methods

Bacterial Strains and Plasmids

The *E. coli* strain BL21(DE3) [F′ *ompT* [lon] $hsdS_B(r_B^- m_B^-)$ *gal dcm* λDE3] (New England Biolabs, Ipswich, MA, USA) was transformed with the pPro24-GFP plasmid (2-methylcitrate inducible, pBR322 origin of replication, *GFPuv* gene, ampicillin resistance).[19] This plasmid contains the propionate-inducible promoter from *S. enterica* that drives the expression of the *GFP* gene in response to propionate.

Culture Conditions

Standard Flask Protocol

Transformed *E. coli* were initially cultured in Luria–Bertani (LB) medium (Sigma-Aldrich, St. Louis, MO, USA) supplemented with 100 μg/mL ampicillin (Gibco; Thermo Fisher Scientific, Waltham, MA, USA) overnight at 37°C with shaking at 120 revolutions per minute (rpm). Next, 200-mL flasks containing 5 mL of LB medium containing ampicillin were inoculated with 500 μL of the overnight culture (1:10 dilution). When these cultures reached an optical density at 600 nm (OD_{600}) of 0.6, they were induced with various propionate concentrations (see the *Propionate Induction* section) and incubated at 37°C with shaking at 120 rpm for 24 hours.

Low-Volume Eppendorf Tube Protocol

To establish a protocol suitable for limited sample volumes, cultures were first grown in flasks to an OD_{600} of 0.6. Next, 75 μL of the culture was transferred to a 1.5 mL Eppendorf tube containing 750 μL of LB medium containing ampicillin (1:10 dilution). This volume was selected to ensure a sufficient sample volume for subsequent assays: 200 μL for fluorometric measurements (according to the Qubit manufacturer's recommendations) and 500 μL for flow cytometry, an amount necessary to obtain at least 2×10^4 target events per acquisition, as described in the sections below. Propionate was added at various concentrations (see the *Propionate Induction* section), and the Eppendorf tubes were then incubated in a ThermoMixer® (Eppendorf, Hamburg, Germany) at 37°C with shaking at 900 rpm for 24 hours.

DMEM Culture Protocol

To evaluate the bacterial biosensor's performance in mammalian cell culture medium, transformed *E. coli* were grown in Dulbecco's modified Eagle medium (DMEM; Gibco, Thermo Fisher Scientific). Approximately 90,000 *E. coli* cells were inoculated into 24-well plates containing 1 mL of DMEM supplemented with 5% fetal bovine serum (Gibco, Thermo Fisher Scientific) and ampicillin (100 μg/mL; Sigma-Aldrich). Then, propionate was added at various concentrations (see the *Propionate Induction* section), and the cultures were incubated at 37°C in a 5% carbon dioxide atmosphere without agitation for 24 hours.

Propionate Induction

Propionate (sodium propionate; Sigma-Aldrich) was prepared as a 1 M stock solution in sterile water, filter-sterilized (0.22 μm), and stored at 4°C. For the dose–response experiments, propionate was added to cultures at final concentrations of 0.1, 0.5, 1, 5, 10, 20, and 50 mM. An equivalent volume of sterile water was added to the control cultures.

Flow Cytometry

Sample Preparation

After the induction period, the *E. coli* cells were processed for flow cytometry as previously described.[36-38] For flask cultures, 800 μL of the culture was harvested and washed with commercially available 1× phosphate-buffered saline (PBS; Gibco, Thermo Fisher Scientific). Next, the cells were fixed with 4% paraformaldehyde (PFA; Sigma-Aldrich) in PBS for 45 minutes at room temperature in the dark. This PFA fixation protocol is widely used for bacterial flow cytometry analysis and preserves fluorescence signal intensity without substantial loss compared to live cells.[39] For Eppendorf tube cultures, the entire fixation procedure was performed in the tube. Finally, the cells were washed twice with 1 mL of 1× PBS, and the pellet was resuspended in 1 mL of PBS for analysis.

Instrument Settings and Data Acquisition

A total of 2×10^4 cells were acquired using a FACSVerse™ flow cytometer (BD Biosciences, San Jose, CA, USA) calibrated with 3-μm beads. The argon laser was set to an excitation wavelength of 488 nm, and GFP fluorescence was detected in the FL1 channel (515–545 nm). Forward scatter (FSC) was detected with a photodiode and an amplification factor E00 and processed using logarithmic gain. Side scatter (SSC) was detected from logarithmic gain using a photomultiplier tube set at 350 V. Briefly, the analysis strategy consisted of gating singlets based on a dot plot comparing FSC area (FSC-A) to FSC height (FSC-H) to exclude aggregates, followed by selecting the main bacterial population based on FSC-A versus SSC area (SSC-A) to remove debris and outliers. The GFP-negative cell population was defined using *E. coli* BL21(DE3) cells lacking the pPro24-GFP plasmid (Supplemental Figure 1A). The GFP-positive cell population was defined using *E. coli* BL21(DE3) cells containing the pPro24-GFP plasmid induced with propionate (Supplemental Figure 1B). The data were analyzed using FlowJo software (version 10.0.7; FlowJo LLC, Ashland, OR, USA).

Fecal Sample Processing and Mock Sample Preparation

Fecal Sample Processing

All participants gave their written informed consent prior to sample collection. Fecal samples from healthy volunteers were processed as previously described.[38,40] Briefly, 1 g of feces was diluted 1:10 in cold sterile PBS and vigorously vortexed for 15 minutes to homogenize and detach bacteria from fecal particles. Next, to separate bacteria from fecal matter and intestinal epithelial cells, the samples were centrifuged at 200 x *g* for two minutes, and 0.5 mL of supernatant was transferred to a new microcentrifuge tube. Then, one volume of cold sterile PBS was added, and the sample was vigorously shaken for 10 minutes. Finally, the samples were centrifuged at 200 x *g* for two minutes to collect the supernatant, then at 8,000 x *g* to harvest the bacterial cells, which were then washed three times with cold sterile PBS and fixed with 4% PFA. This methodology yields approximately 10^9 cells/mL independent of the initial dilution.

Mock IBS-D Sample

For proof of concept, mock samples prepared from processed fecal samples from healthy volunteers, as described above, were spiked with propionate to a final concentration of 100 mM, the upper end of the reported range in patients with IBS-D, to evaluate the bacterial biosensor's response to elevated propionate levels. These mock samples were incubated with the bacterial biosensor (1:1 ratio) for 24 hours at 37°C with gentle agitation, followed by flow cytometry analysis as described in the *Flow Cytometry* section. All experiments were performed with three independent biological replicates per condition, each measured in triplicate.

Fluorometric Measurements

The GFP fluorescence of PFA-fixed bacteria was measured in 200 μL samples in manufacturer-provided 0.5 mL Qubit® assay tubes using a Qubit® 3.0 fluorometer (Thermo Fisher Scientific) with blue excitation (470 nm) and green emission (510–580 nm) settings. The blank for each measurement consisted of 1× PBS. Each sample was examined in three technical

replicates, and the mean fluorescence intensity (MFI, in arbitrary units [AU]) was calculated. For all assays, three independent biological replicates were analyzed per condition, each measured in triplicate.

Biosensor Growth Kinetics

To determine biosensor growth kinetics in different media, serial culture dilutions were plated on LB agar plates supplemented with ampicillin (100 μg/mL). The plates were incubated overnight at 37°C, after which colonies were counted, and the number of colony-forming units (CFUs) per mL was calculated based on dilution factors and plating volumes.

Statistical Analysis

All experiments were performed with three biological replicates, each measured in triplicate (technical replicates). Statistical analyses were performed using GraphPad Prism for Mac OS X (version 9.2; GraphPad Software, San Diego, CA, USA), and a p-value < 0.05 was considered statistically significant. Continuous variables are presented as mean ± standard deviation (SD) or standard error of the mean (SEM) as indicated. They were compared between two groups using Student's t-test and between more than two groups using one-way analysis of variance (ANOVA) followed by post-hoc Tukey's tests. The bacterial biosensor's diagnostic performance was assessed using receiver operating characteristic (ROC) curves. The agreement between propionate concentration and fluorescence intensity was evaluated using Cohen's κ coefficient.

Results

Biosensor Growth Kinetics and Performance in Different Culture Media

To evaluate the bacterial biosensor's applicability for diagnostic purposes and translational research, the growth and fluorescence output of *E. coli* cells containing the pPro24-GFP plasmid in DMEM, a mammalian cell culture medium that differs substantially from standard bacterial growth media in composition (amino acids, vitamins, inorganic salts, D-glucose, and phenol red *vs.* tryptone, sodium chloride, and yeast extract in LB), was first evaluated. Biosensor growth kinetics differed between DMEM and LB medium (Supplemental Figure 2). The LB cultures reached approximately 1.8×10^{10} CFU/mL (2^{34}) after 48 hours of incubation, whereas the DMEM cultures reached approximately 4.5×10^{9} CFU/mL (2^{32}) after 120 hours.

Dose–response experiments with propionate concentrations ranging from 0.5 to 50 mM showed that the fluorescence intensity was comparable in DMEM and LB medium (Figure 1). This finding indicates that the biosensor maintains functionality across different culture media, a critical feature for potential diagnostic applications involving diverse sample

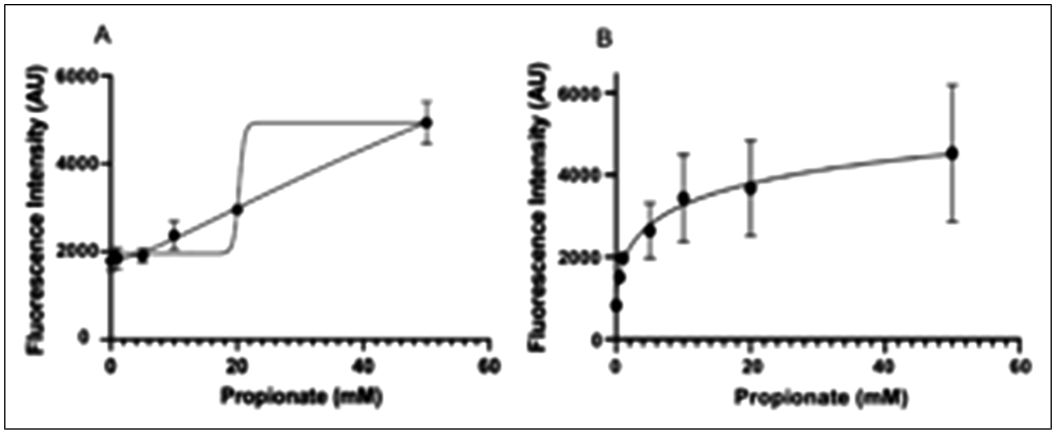

Figure 1. Dose–response curves for bacterial biosensors grown in flasks and Eppendorf tubes. (A) The bacterial biosensor was grown in LB medium in 50-mL flasks for 6 hours at 37°C with constant shaking at 130 rpm. The cells were exposed to increasing propionate concentrations (0.5, 1, 5, 10, 20, and 50 mM) for 24 hours, with 1× PBS used as a control. (B) The bacterial biosensor was grown for 24 hours at 37°C with constant shaking at 900 rpm in a ThermoMixer® using 750 μL of LB medium inoculated with 75 μL of a biosensor culture ($OD_{600} = 0.7$). It was then exposed to the same propionate concentrations as in (A). In both experiments, after induction, the cells were fixed with 4% PFA for 30 minutes and then resuspended in 1 × PBS before fluorescence measurement. Data represent the mean ± SD of three independent samples and were compared using one-way ANOVA followed by post-hoc Tukey's tests

types. Thus, despite the reduced growth rate and lower final cell density in DMEM, the bacterial biosensor produced sufficient fluorescence for reliable detection. However, its performance in clinically relevant gut-like media remains to be established.

Validation With Complex Biological Samples

To assess the bacterial biosensor's potential for clinical diagnostics, particularly for detecting elevated propionate levels in fecal samples from patients with IBS-D, background fluorescence and potential interference from sample components were first characterized.

Autofluorescence Assessment

The processed fecal samples from healthy volunteers exhibited negligible autofluorescence when analyzed by flow cytometry using the same detection parameters employed for GFP (Supplemental Figure 3A). Propionate alone showed no intrinsic fluorescence under these conditions (Supplemental Figure 3B), confirming that fluorescence signals arise exclusively from GFP expression in the bacterial biosensor.

Mock IBS-D Sample Analysis

In mock fecal samples designed to mimic IBS-D conditions (healthy fecal samples supplemented with 100 mM propionate), biosensor fluorescence was successfully detected by flow cytometry (Figure 2). The fluorescent signal was clearly distinguishable from the background, demonstrating the bacterial biosensor's ability to detect elevated propionate levels in complex biological matrices. This proof-of-concept result suggests the biosensor's potential utility for detecting changes in propionate levels associated with disease states in clinical samples.

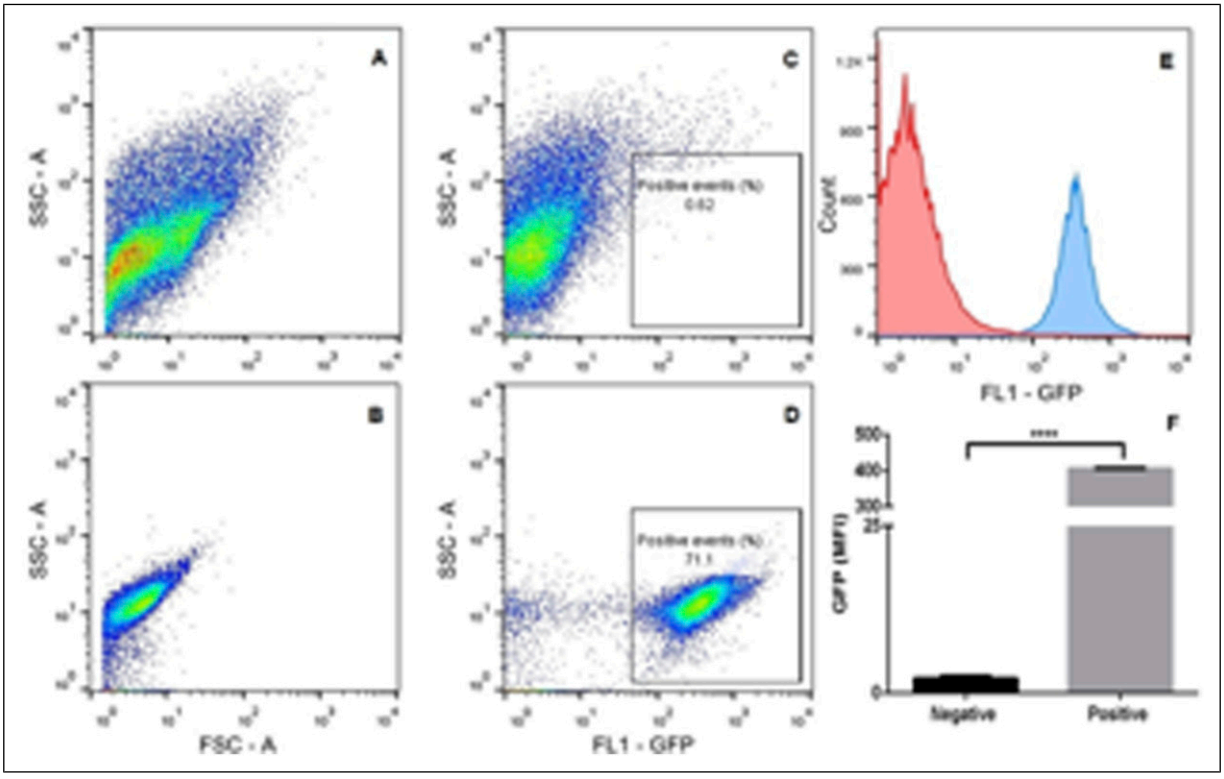

Figure 2. Flow cytometry of the bacterial biosensor response in mock IBS-D samples. (A) Dot plot of FSC-A versus FSC-H showing gating of singlets to exclude aggregates. (B, C) Dot plots of FSC-A versus SSC-A showing the bacterial population in the absence (B) and presence (C) of the bacterial biosensor. (D) GFP fluorescence was assessed in the FL1 channel, revealing only 0.6% GFP-positive events in the absence of the bacterial biosensor, indicating minimal background signal. (E) Mock IBS-D samples showed a marked increase to 71% GFP-positive events upon addition of the bacterial biosensor. (F) Representative histograms of GFP fluorescence comparing samples with (blue) and without (red) the bacterial biosensor. Data represent the mean ± SD of three biological replicates and were compared using the Mann–Whitney U test. Significance: ****, $p < 0.0001$

Development of a Low-Volume Protocol for Portable Fluorometry

A primary objective of this study was to establish a standardized protocol for processing low-volume biological samples using readily accessible instrumentation. Clinical samples are often limited in volume (30–80 μL), necessitating methods that minimize sample requirements while maintaining reliability and reproducibility.

A protocol was developed using 1.5 mL Eppendorf tubes containing 750 μL of culture medium (Figure 3A) inoculated with 75 μL (1:10 dilution) of biosensor culture ($OD_{600} = 0.7$) and supplemented with propionate. After 24 hours of incubation at 37°C with shaking at 900 rpm in a ThermoMixer®, the cultures reached an OD_{600} of 1.2, comparable to the cell density achieved in flask cultures after six hours of incubation.

Both flow cytometry and Qubit® fluorometry detected quantifiable signals under these conditions. However, the detection threshold increased to 10 mM propionate in the low-volume format (Figure 3B), compared to 0.1 mM for flask cultures (Figure 3A). This increase in detection threshold reduces the biosensor's sensitivity. It likely reflects a smaller percentage of propionate-responding cells: approximately 30% of the *E. coli* cells fluoresced in the Eppendorf tubes, compared with approximately 80% in the flask cultures.

Despite this limitation, the Qubit®-based measurements demonstrated excellent reproducibility, offering a more time- and resource-efficient alternative to flow cytometry for routine sample analysis. The portable nature of the Qubit® fluorometer makes this approach particularly suitable for point-of-care or resource-limited settings.

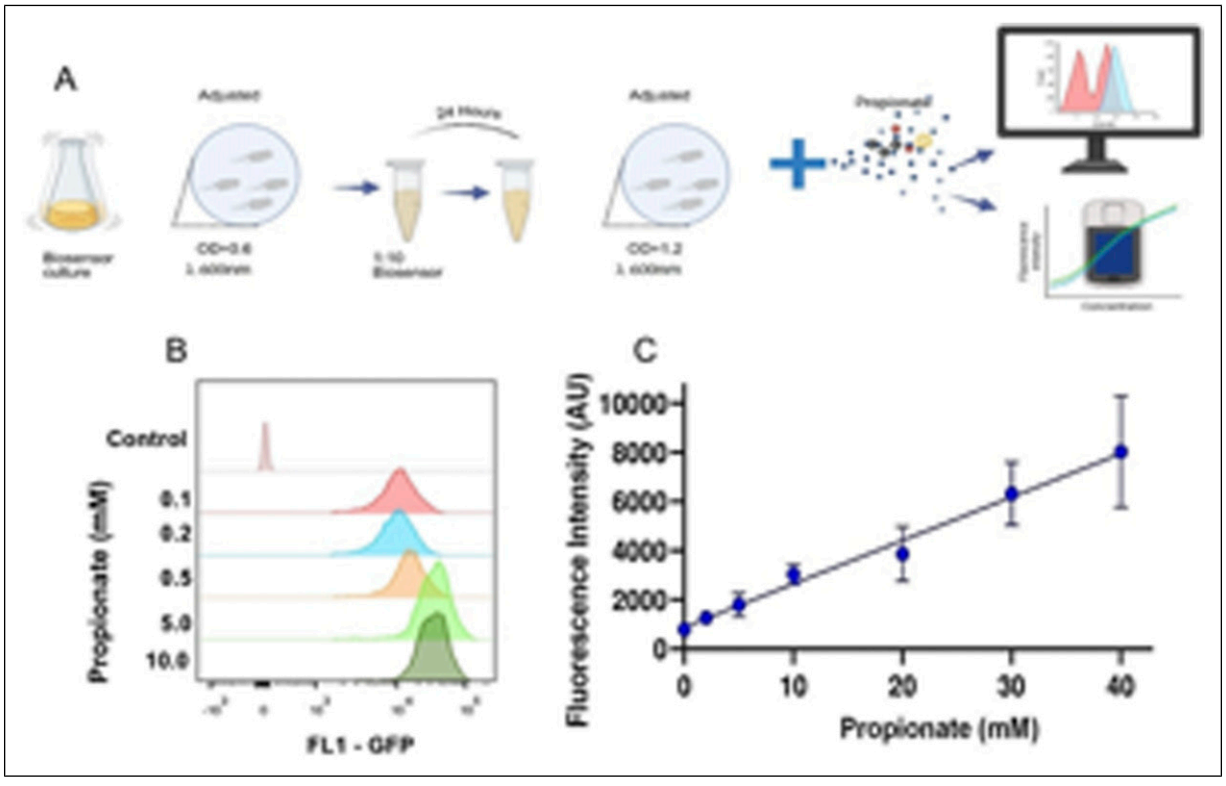

Figure 3. The low-volume Eppendorf tube protocol and comparison of detection thresholds and responses between flask and Eppendorf tube cultures. (A) Biosensor cultures were initially grown overnight in LB medium with shaking until the OD_{600} reached 0.6. Next, 75 μL of the culture was transferred to an Eppendorf tube, diluted 1:10 with LB medium, incubated until the OD_{600} reached 1.2, and then supplemented with propionate at the indicated concentrations and incubated for 24 hours. Following incubation, GFP fluorescence was quantified by flow cytometry. (B) Flow cytometry histograms obtained under standard flask culture conditions, showing GFP fluorescence of biosensor cells after 24 hours of exposure to increasing propionate concentrations (0.1, 0.2, 0.5, 5, and 10 mM). (C) Dose–response curve showing MFI (in AU) as a function of the propionate concentration for biosensor cultures using the low-volume Eppendorf protocol. Data represent the mean ± SD of three independent samples and were compared using one-way ANOVA followed by post-hoc Tukey's tests

Assessment of Diagnostic Performance

The bacterial biosensor's diagnostic utility was evaluated using ROC curve analysis of fluorescence intensity (in AU) versus propionate concentration. This analysis yielded a Cohen's κ coefficient of 0.716, indicating substantial agreement between measured fluorescence and propionate levels. The bacterial biosensor exhibited a sensitivity of 71% and specificity of 86% (Figure 4). This level of agreement suggests that the bacterial biosensor could reliably distinguish between samples with different propionate concentrations, supporting its potential application in clinical diagnostics where semi-quantitative or threshold-based detection may be sufficient for decision-making.

Discussion

Clinical Significance of Propionate Detection

The ability to detect propionate in biological samples has clinical implications across multiple disease contexts. In the gastrointestinal tract, elevated propionate levels have been associated with Crohn's disease, IBS-D, and vascular calcification.[22,26,27] In the oral cavity, high propionate levels correlate with periodontal disease.[28] In the central nervous system, propionate has been proposed as a potential contributor to increased risk for Alzheimer's disease through mechanisms involving penetration of the blood-brain barrier, although this link currently remains associative.[29-31] These associations highlight the value of accessible propionate detection tools for improving the diagnosis and management of various diseases and conditions.

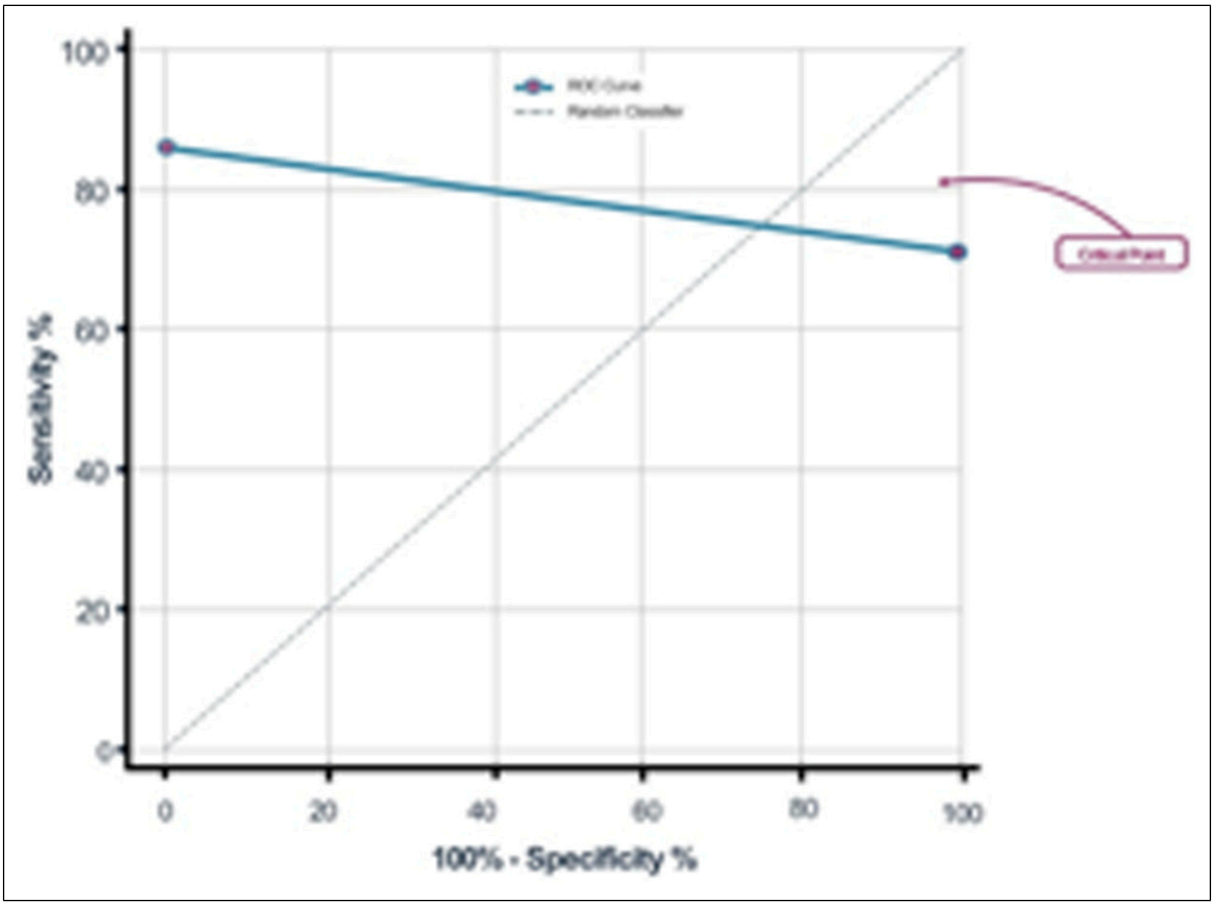

Figure 4. Diagnostic performance of the bacterial propionate biosensor. The ROC curve shows the correlation between the MFI (in AU) of GFP measured by flow cytometry and the Qubit® (in AU). The analysis yielded a Cohen's κ coefficient of 0.716, sensitivity of 71%, and specificity of 86%. The ROC curve was constructed from three independent experiments, each measured in triplicate

Advantages of Microbial Biosensors for Propionate Detection

Current gold-standard methods for propionate quantification, such as GC-MS and HPLC, have high sensitivity and specificity but require expensive instrumentation, technical expertise, and substantial sample volumes. The bacterial biosensor presented here offers numerous advantages over these methods:

1. **Cost-effectiveness.** The biosensor utilizes standard bacterial culture techniques and reagents, with optional readout via portable fluorometry rather than specialized analytical equipment.
2. **Simplicity.** The biosensor protocol requires minimal technical training and can be performed in basic laboratory settings.
3. **Low Sample Volume Requirement.** The optimized biosensor protocol accommodates sample volumes as small as 750 μL, suitable for clinical specimens that are often limited in quantity.
4. **Versatility.** The biosensor can function across multiple culture media, enabling adaptation to diverse sample matrices.
5. **Portability.** The biosensor can be evaluated using a handheld fluorometer (Qubit® 3.0), enabling point-of-care applications and deployment in resource-limited settings.

Biosensor Performance Across Culture Conditions

Our results demonstrate that the bacterial propionate biosensor remains functional in both LB medium and DMEM, despite substantial compositional differences. The comparable fluorescence intensities (3863 ± 957 AU) achieved in both media indicate robust performance across nutritional environments. This versatility is crucial for diagnostic applications, where sample matrices may vary considerably.

The reduced *E. coli* growth rate in DMEM (120 hours to the early stationary phase *vs.* 48 hours in LB) reflects its optimization for mammalian rather than bacterial cell culture. Nevertheless, the bacterial biosensor produced a fluorescence signal sufficient for reliable detection, demonstrating its utility even under suboptimal growth conditions, and exhibited a concentration–signal relationship, suggesting that it could be used to segregate cases and/or differentiate among various states along a gradient.

Low-Volume Protocol Development and Trade-offs

The development of a low-volume protocol suitable for clinical samples was a key objective of this study. While the Eppendorf tube format successfully reduced sample requirements to 750 μL, this came at the cost of reduced sensitivity (10 mM detection threshold *vs.* 0.1 mM in flask cultures) and a lower response rate (~30% *vs.* ~80% of cells fluorescing). Several factors likely contributed to this reduced performance:

1. **Oxygen Availability.** The higher surface-area-to-volume ratio of flasks may provide better aeration, supporting more robust bacterial metabolism and gene expression.
2. **Mixing Efficiency.** Orbital shaking of flasks provides more uniform mixing than linear shaking in a ThermoMixer®, potentially affecting the nutrient distribution and propionate accessibility.
3. **Cell Density Effects.** The lower final cell density in Eppendorf tubes may result in reduced quorum-sensing effects or other density-dependent phenomena that influence gene expression.

Validation With Complex Biological Samples

The successful detection of an elevated propionate level in mock fecal samples provides essential proof-of-concept evidence for clinical applications. The negligible autofluorescence of processed fecal samples and the lack of intrinsic propionate fluorescence confirmed that the fluorescence signals derived exclusively from biosensor GFP expression, minimizing false-positive results.

The mock IBS-D samples (healthy feces + 100 mM propionate) demonstrated a clear fluorescence signal above background, validating the bacterial biosensor's ability to function in complex biological matrices containing diverse microbial communities, metabolites, and particulate matter. This finding supports the feasibility of applying the bacterial biosensor to actual patient samples, although additional validation with authentic clinical specimens will be necessary.

Despite these limitations, the 10 mM detection threshold remains clinically relevant. In healthy individuals, luminal propionate levels in the gut range from 10 to 30 mM, reflecting basal SCFA production under homeostatic conditions.[28] In

contrast, recent meta-analyses and reviews indicate that pathological conditions, including IBS-C and IBS-D, are characterized by deviations from this physiological range; for example, fecal propionate levels can exceed 100 mM in patients with IBS-D, whereas they are significantly lower in patients with IBS-C than in healthy controls. This bidirectional dysregulation underscores the value of our bacterial propionate biosensor as a tool capable of detecting both high and low propionate levels associated with pathological conditions. The 10 mM detection threshold situates the bacterial biosensor at the clinically relevant transition point between eubiotic and dysbiotic propionate levels. For diagnostic applications where threshold-based classification is sufficient, this sensitivity is adequate.

In our experiments, GFP fluorescence was measured after 24 hours of propionate exposure, which provided robust signals. Notably, our mock IBS-D experiment showed a high GFP fluorescence signal at this time point. Consistent with this result, a related pPro24-based biosensor showed GFP fluorescence responses that were clearly different across propionate concentrations after 6 hours of growth, with stable dose–response parameters observed between 14–16 hours, indicating that detection is feasible across a range of incubation times.[21]

Diagnostic Performance and Clinical Utility

The ROC curve analysis yielded a Cohen's κ coefficient of 0.716, indicating substantial agreement between fluorescence intensity and propionate concentration. In clinical diagnostics, Cohen's κ coefficients of 0.61–0.80 are generally considered to represent significant agreement, while those above 0.80 indicate almost perfect agreement. While further optimization may improve this metric, the biosensor's current performance suggests utility for semi-quantitative applications such as:

1. **Screening.** Identifying patients with elevated propionate levels who may benefit from a more thorough diagnostic workup.
2. **Monitoring.** Monitoring changes in propionate production during disease progression or therapeutic intervention.
3. **Research.** Investigating the relationships between propionate levels and clinical outcomes in large cohorts where high-throughput, cost-effective methods are essential.

Broader Applications Beyond Clinical Diagnostics

Beyond clinical diagnostics, the bacterial propionate biosensor has potential applications in:

1. **Food Safety and Quality Control.** Detecting propionate produced by spoilage organisms[41-43] or contaminants in food and beverages.[44]
2. **Microbiome Research.** Studying propionate production by specific bacterial species or communities under various conditions.
3. **Metabolic Engineering.** Monitoring propionate levels in engineered bacterial strains for industrial applications.
4. **Environmental Monitoring.** Assessing propionate levels in environmental samples where this metabolite serves as an indicator of microbial activity.

Study Limitations

This study had several limitations that should be acknowledged:

1. **Detection Threshold.** The 10 mM detection threshold in the low-volume format may not be suitable for all applications, particularly those requiring the detection of lower propionate concentrations.
2. **Response Time.** The 24-hour incubation period required by the low-volume protocol may be too long for some clinical scenarios requiring rapid results. In addition, the minimum incubation time required for reliable detection of propionate concentrations was not determined.
3. **Sample Processing.** While effective, the fecal sample processing protocol adds complexity and time to the overall workflow.
4. **Limited Clinical Validation.** While mock sample experiments demonstrated proof of concept, an important limitation is that only a single representative high propionate concentration (100 mM) was tested in the mock fecal samples, which reflected the upper limit of the range observed in patients with IBS-D. Future studies should include dose–response experiments across the clinically relevant concentration range to determine the bacterial biosensor's limits of detection and sensitivity. Validation with real fecal samples from patients with different intestinal diseases is also necessary before clinical implementation.

5. **Biosensor Specificity.** While the propionate-inducible promoter system is well characterized and previous research has shown no significant induction in response to acetate or butyrate, potential cross-reactivity with these molecules was not evaluated under the conditions tested here and should be investigated in future studies.
6. **Limited Evaluation in Clinically Relevant Intestinal Media.** Although the bacterial biosensor showed comparable performance in standard media such as LB medium and DMEM and demonstrated functionality in mock fecal samples, it was not evaluated in more physiologically relevant gut-like conditions, such as anaerobic intestinal simulation media or media supplemented with fecal extracts. This omission limits the interpretation of the current findings and should be addressed in future studies.
7. **Host Strain Endogenous Propionate Metabolism.** *E. coli* strain BL21(DE3) was selected for its well-characterized genetics, high transformation efficiency, and extensive use in biosensor applications. However, it carries the chromosomal *prp* operon, which mediates propionate catabolism through the 2-methylcitrate pathway, potentially depleting propionate and interfering with biosensor performance. Moreover, it can metabolize alternative carbon sources that generate propionyl–coenzyme A, which is converted to 2-methylcitrate, the co-activator of PrpR, and could therefore contribute to basal GFP expression. Notably, in our experiments, control cultures without propionate exhibited comparable basal GFP fluorescence in both tested media, consistent with PprpB suppression in glucose-supplemented media. A key experiment that remains to be performed is the use of *prp* knockout strains, which were not evaluated in this study. Future studies should evaluate their use to elucidate the contribution of this variable and to determine if eliminating endogenous propionate catabolism improves biosensor sensitivity.
8. **Quantitative Performance of the Qubit® fluorometer.** Qubit® 3.0 lacks user-adjustable gain and bandwidth settings, restricting its optimization for GFP samples, and its linear dynamic range is narrower than that of microplate readers. Unlike flow cytometry, which measures fluorescence at the individual-cell level, the Qubit® integrates the entire signal from the suspension. However, these limitations were mitigated through standardization experiments, and the ROC curve analysis (Cohen's κ coefficient = 0.716) demonstrates acceptable diagnostic performance despite these limitations.
9. **Biosensor Stability and Shelf Life.** The long-term viability of the bacterial propionate biosensor was not formally evaluated in this study. While cryopreservation in glycerol stocks is a standard method for preserving recombinant *E. coli* viability and plasmid retention for up to 10 years,[45] this approach requires cold-chain infrastructure that may not be universally available. Alternative preservation strategies, such as lyophilization, represent a potential option to optimize the stability and accessibility of the biosensor and should be evaluated in future studies.

Future Directions

Several avenues for future development could enhance the bacterial biosensor's performance and expand its applications:

1. **Enhanced Sensitivity.** Engineering approaches such as promoter optimization, the use of brighter fluorescent proteins, or signal amplification strategies could lower the detection threshold.
2. **Reduced Response Time.** Exploring faster-growing bacterial strains, standardized alternative detection strategies, and optimized incubation times could significantly reduce the response time, making the assay more suitable for clinical applications.
3. **Multiplexing.** Developing biosensors that can simultaneously detect multiple SCFAs (acetate, propionate, and butyrate) would provide more comprehensive metabolic profiles.
4. **Clinical Validation.** The bacterial biosensor should be systematically evaluated with patient samples across multiple disease states and compared with gold-standard analytical methods. Evaluating its performance in fecal samples in a dose–response range (20–40 mM) would enhance its translational potential.
5. **Develop a Point-of-care Device.** Integration of the bacterial biosensor with microfluidic systems or other miniaturized platforms could enable true point-of-care applications.
6. **Quantitative Calibration.** Development of standardized calibration protocols and reference materials would enable more precise quantification.
7. **Optimize Biosensor Stability.** Evaluate alternative preservation strategies, including cryopreservation and lyophilization, and quantify bacterial biosensor performance under these storage conditions.

Conclusions

This study presents an optimized protocol for a bacterial biosensor for propionate capable of detecting millimolar concentrations in low-volume samples across different culture media. The protocol is cost-effective, easy to use, and provides

consistent, reproducible results using a portable fluorometer (Qubit® 3.0), making it accessible for diverse laboratory settings.

The results demonstrated that the biosensor remains functional in both standard bacterial (LB) and mammalian (DMEM) cell culture medium, achieving comparable fluorescence intensities despite substantial differences in composition. The development of a low-volume protocol (750 μL) suitable for clinical specimens represents an important advance. However, there is a trade-off in sensitivity (detection threshold of 10 mM *vs.* 0.1 mM in standard flask cultures).

Proof-of-concept experiments with mock fecal samples successfully demonstrated the biosensor's ability to detect elevated propionate at levels typically found in patients with IBS-D, with negligible background interference from sample autofluorescence or intrinsic propionate fluorescence. ROC curve analysis yielded a Cohen's κ coefficient of 0.716, indicating substantial agreement between fluorescence intensity and propionate concentration, supporting potential diagnostic applications.

The clinical significance of propionate detection extends across multiple disease contexts, including gastrointestinal disorders (IBS-D and Crohn's disease), periodontal disease, and potentially neurodegenerative conditions such as Alzheimer's disease. The accessibility and affordability of this bacterial biosensor-based approach could facilitate wider implementation of propionate monitoring in clinical settings, potentially improving diagnosis, disease management, and therapeutic monitoring.

While further optimization and clinical validation are necessary, this study establishes a proof-of-concept for the detection of propionate in biological samples. The standardized protocol and use of portable instrumentation offer a promising basis for researchers and clinicians seeking to understand the role of propionate in health and disease, with the potential to enhance future applications in clinical diagnostics and research.

Acknowledgments

Salvador Fabela and Camilo Pablo Martínez Reyes received postdoctoral fellowships from the Dirección General de Asuntos del Personal Académico at Universidad Nacional Autónoma de México. The authors thank Lilia Nathalie Jiménez Guzmán for her technical support on this project.

Ethical Considerations

This study was approved by the Investigation and Ethics Committee of the School of Medicine of the UNAM. (Register number CIE 127/2017, 6/FEB/2018).

Consent to Participate

All participants gave their written informed consent prior to sample collection.

Consent for Publication

Not applicable. No identifiable patient images, individual patient data, or case reports are included in the present research.

Author Contributions

Conceptualization, Y. L.-V. and R. A.-H.; methodology, S. F., C.P M.-R., G. C.-R., and P. O.; validation, S. F., C.P. M.-R., G. C.-R., and P. O.; formal analysis, E. G.-H.; resources, Y. L.-V.; writing—original draft, S. F., R. A.-H., G. C.-R., P. O., E. G.-H., and Y. L.-V.; writing—review and editing, C.P. M.-R., R. A.-H., G. C.-R., P. O., E. G.-H., and Y. L.-V.; visualization, S. F. and Y. L.-V.; supervision R. A.-H., G. C.-R., P. O., E. G.-H., and Y. L.-V.; project administration, G. C.-R.; funding acquisition, Y. L.-V. All authors have read and agreed to the published version of the manuscript.

Funding

The authors disclosed receipt of the following financial support for the research, authorship, and/or publication of this article: This research was funded by the Dirección General de Asuntos del Personal Académico-Programa de Apoyo a Proyectos de Investigación e Innovación Tecnológica (grant numbers IT202020, IT200224, and IV200321). No funding bodies were involved in the study's design, data collection and analysis, decision to publish, or manuscript preparation.

Declaration of Conflicting Interests

The authors declared no potential conflicts of interest with respect to the research, authorship, and/or publication of this article.

Data Availability Statement

The data presented in this study are available from the corresponding author upon reasonable request.

Supplemental Material

Supplemental material for this article is available online.

References

1. Louis P, Flint HJ. Formation of propionate and butyrate by the human colonic microbiota. *Environ Microbiol*. 2017;19(1):29-41. doi:10.1111/1462-2920.13589.
2. Louis P, Flint HJ. Diversity, metabolism, and microbial ecology of butyrate-producing bacteria from the human large intestine. *FEMS Microbiol Lett*. 2009;294(1):1-8. doi:10.1111/j.1574-6968.2009.01514.x.
3. Van der Hee B, Wells JM. Microbial regulation of host physiology by short-chain fatty acids. *Trends Microbiol*. 2021;29(8):700-712. doi:10.1016/j.tim.2021.02.001.
4. Portincasa P, Bonfrate L, Vacca M, et al. Gut microbiota and short-chain fatty acids: implications in glucose homeostasis. *Int J Mol Sci*. 2022;23(3):1105. doi:10.3390/ijms23031105.
5. Trøseid M, Andersen GØ, Broch K, Hov JR. The gut microbiome in coronary artery disease and heart failure: Current knowledge and future directions. *EBioMedicine*. 2020;52:102649. doi:10.1016/j.ebiom.2020.102649.
6. Morrison DJ, Preston T. Formation of short-chain fatty acids by the gut microbiota and their impact on human metabolism. *Gut Microbes*. 2016;7(3):189-200. doi:10.1080/19490976.2015.1134082.
7. Silva YP, Bernardi A, Frozza RL. The role of short-chain fatty acids from gut microbiota in gut-brain communication. *Front Endocrinol*. 2020;11:25. doi:10.3389/fendo.2020.00025.
8. Nakanishi N, Tashiro K, Kuhara S, Hayashi T, Sugimoto N, Tobe T. Regulation of virulence by butyrate sensing in enterohaemorrhagic *Escherichia coli*. *Microbiology*. 2009;155(Pt 2):521-530. doi:10.1099/mic.0.023499-0.
9. Takao M, Yen H, Tobe T. LeuO enhances butyrate-induced virulence expression through a positive regulatory loop in enterohaemorrhagic *Escherichia coli*. *Mol Microbiol*. 2014;93(6):1302-1313. doi:10.1111/mmi.12737.
10. Tobe T, Nakanishi N, Sugimoto N. Activation of motility by sensing short-chain fatty acids via a flagellar gene regulatory cascade in enterohemorrhagic *Escherichia coli*. *Infect Immun*. 2011;79(3):1016-1024. doi:10.1128/IAI.00927-10.
11. Hang S, Purdy AE, Robins WP, et al. The acetate switch of an intestinal pathogen disrupts host insulin signaling and lipid metabolism. *Cell Host Microbe*. 2014;16(5):592-604. doi:10.1016/j.chom.2014.10.006.
12. Jacob K, Rasmussen A, Tyler P, et al. Regulation of acetyl-CoA synthetase transcription by the CrbS/R two-component system is conserved in genetically diverse environmental pathogens. *PLoS One*. 2017;12(5):e0177825. doi:10.1371/journal.pone.0177825.
13. Sepulveda E, Lupas AN. Characterization of the CrbS/R two-component system in *Pseudomonas fluorescens* reveals a new set of genes under its control and a DNA motif required for CrbR-mediated transcriptional activation. *Front Microbiol*. 2017;8:2287. doi:10.3389/fmicb.2017.02287.
14. Horswill AR, Escalante-Semerena JC. Propionate catabolism in *Salmonella typhimurium* LT2: two divergently transcribed units comprise the prp locus at 8.5 centisomes, prpR encodes a member of the sigma-54 family of activators, and the prpBCDE genes constitute an operon. *J Bacteriol*. 1997;179(3):928-940. doi:10.1128/JB.179.3.928-940.1997.
15. Horswill AR, Escalante-Semerena JC. *Salmonella typhimurium* LT2 catabolizes propionate via the 2-methylcitric acid cycle. *J Bacteriol*. 1999;181(18):5615-5623. doi:10.1128/JB.181.18.5615-5623.1999.
16. Horswill AR, Escalante-Semerena JC. The *prpE* gene of *Salmonella typhimurium* LT2 encodes propionyl-CoA synthetase. *Microbiology*. 1999;145(Pt 6):1381-1388. doi:10.1099/13500872-145-6-1381.
17. Horswill AR, Escalante-Semerena JC. In vitro conversion of propionate to pyruvate by *Salmonella enterica* enzymes: 2-methylcitrate dehydratase (PrpD) and aconitase enzymes catalyze the conversion of 2-methylcitrate to 2-methylisocitrate. *Biochemistry*. 2001;40(15):4703-4713. doi:10.1021/bi015503b.
18. Horswill AR, Escalante-Semerena JC. Characterization of the propionyl-CoA synthetase (PrpE) enzyme of *Salmonella enterica:* residue Lys592 is required for propionyl-AMP synthesis. *Biochemistry*. 2002;41(7):2379-2387. doi:10.1021/bi015647q.
19. Lee SK, Keasling JD. A propionate-inducible expression system for enteric bacteria. *Appl Environ Microbiol*. 2005;71(11):6856-6862. doi:10.1128/AEM.71.11.6856-6862.2005.
20. Lebovich M, Andrews LB. Surveying the genetic design space for transcription factor-based metabolite biosensors: synthetic gamma-aminobutyric acid and propionate biosensors in *E. coli* Nissle 1917. *Front Bioeng Biotechnol*. 2022;10:938056. doi:10.3389/fbioe.2022.938056.
21. Serebrinsky-Duek K, Barra M, Garrido D. Engineered bacteria for short-chain-fatty-acid-repressed expression of biotherapeutic molecules. *Microbiol Spectr*. 2023;11(2):e0004923. doi:10.1128/spectrum.00049-23.

22. Bajic D, Niemann A, Hillmer A-K, et al. Gut microbiota-derived propionate regulates the expression of Reg3 mucosal lectins and ameliorates experimental colitis in mice. *J Crohns Colitis*. 2020;14(10):1462-1472. doi:10.1093/ecco-jcc/jjaa065.
23. Su J, Braat H, Peppelenbosch MP. Gut microbiota-derived propionate production may explain beneficial effects of intermittent fasting in experimental colitis. *J Crohns Colitis*. 2021;15(6):1081-1082. doi:10.1093/ecco-jcc/jjaa248.
24. Yan J, Pan Y, Shao W, et al. Beneficial effect of propionate on vascular calcification through intestinal microbiota remodelling. *Microbiome*. 2022;10(1):195. doi:10.1186/s40168-022-01390-0.
25. Chambers ES, Viardot A, Psichas A, et al. Effects of targeted delivery of propionate to the human colon on appetite regulation, body weight maintenance and adiposity in overweight adults. *Gut*. 2015;64(11):1744-1754. doi:10.1136/gutjnl-2014-307913.
26. Hosseini E, Grootaert C, Verstraete W, Van de Wiele T. Propionate as a health-promoting microbial metabolite in the human gut. *Nutr Rev*. 2011;69(5):245-258. doi:10.1111/j.1753-4887.2011.00388.x.
27. Marzocco S, Fazeli G, Micco LD, et al. Supplementation of sodium propionate in patients on maintenance hemodialysis: Beneficial effects on inflammatory parameters and gut-derived uremic toxins, a pilot study (PLAN Study). *J Clin Med*. 2018;7(10):315. doi:10.3390/jcm7100315.
28. Cummings JH, Beatty ER, Kingman SM, Bingham SA, Englyst HN. Digestion and physiological properties of resistant starch in the human large bowel. *Br J Nutr*. 1996;75(5):733-747. doi:10.1079/BJN19960177.
29. Sun Q, Jia Q, Song L, Duan L. Alterations in fecal short-chain fatty acids in patients with irritable bowel syndrome. *Medicine (Baltimore)*. 2019;98(7):e14513. doi:10.1097/MD.0000000000014513.
30. Pobeguts OV, Ladygina VG, Evsyutina DV, et al. Propionate induces virulent properties of Crohn's disease-associated *Escherichia coli*. *Front Microbiol*. 2020;11:1460. doi:10.3389/fmicb.2020.01460.
31. Aimetti M, Cacciatore S, Graziano A, Tenori L. Metabonomic analysis of saliva reveals a generalized chronic periodontitis signature. *Metabolomics*. 2011;8(3):465-474. doi:10.1007/S11306-011-0331-2.
32. Chen CK, Wu YT, Chang YC. Association between chronic periodontitis and the risk of Alzheimer's disease: a retrospective, population-based, matched-cohort study. *Alzheimers Res Ther*. 2017;9(1):56. doi:10.1186/s13195-017-0282-6.
33. Kamer AR, Pirraglia E, Tsui W, et al. Periodontal disease associates with higher brain amyloid load in normal elderly. *Neurobiol Aging*. 2015;36(2):627-633. doi:10.1016/j.neurobiolaging.2014.10.038.
34. Killingsworth J, Sawmiller D, Shytle RD. Propionate and Alzheimer's disease. *Front Aging Neurosci*. 2020;12:580001. doi:10.3389/fnagi.2020.580001.
35. Haijes HA, van Hasselt PM, Jans JJM, Verhoeven-Duif NM. Pathophysiology of propionic and methylmalonic acidemias. Part 2: Treatment strategies. *J Inherit Metab Dis*. 2019;42(5):745-761. doi:10.1002/jimd.12128.
36. Valdivia RH, Falkow S. Bacterial genetics by flow cytometry: rapid isolation of *Salmonella typhimurium* acid-inducible promoters by differential fluorescence induction. *Mol Microbiol*. 1996;22(2):367-378. doi:10.1046/j.1365-2958.1996.00120.x.
37. Valdivia RH, Hromockyj AE, Monack D, Ramakrishnan L, Falkow S. Applications for green fluorescent protein (GFP) in host-pathogen interactions. *Gene*. 1996;173(1 Spec No):47-52. doi:10.1016/0378-1119(95)00706-7.
38. Bruder LM, Dörkes M, Fuchs BM, Ludwig W, Liebl W. Flow cytometric sorting of fecal bacteria after in situ hybridization with polynucleotide probes. *Syst Appl Microbiol*. 2016;39(7):464-475. doi:10.1016/j.syapm.2016.08.005.
39. Telford WG, Hawley T, Subach F, Verkhusha V, Hawley RG. Flow cytometry of fluorescent proteins. *Methods*. 2012;57(3):318-330. doi:10.1016/j.ymeth.2012.01.003.
40. Aymanns S, Mauerer S, van Zandbergen G, Wolz C, Spellerberg B. High-level fluorescence labeling of Gram-positive pathogens. *PLoS One*. 2011;6(6):e19822. doi:10.1371/journal.pone.0019822.
41. Textor S, Wendisch VF, De Graaf AA, et al. Propionate oxidation in *Escherichia coli*: evidence for operation of a methylcitrate cycle in bacteria. *Arch Microbiol*. 1997;168(5):428-436. doi:10.1007/s002030050518.
42. Brock M, Maerker C, Schütz U, Völker U, Buckel W. Oxidation of propionate to pyruvate in *Escherichia coli*. Involvement of methylcitrate dehydratase and aconitase. *Eur J Biochem*. 2002;269(24):6184-6194. doi:10.1046/j.1432-1033.2002.03336.x.
43. Evans CT, Sumegi B, Srere PA, Sherry AD, Malloy CR. [13C] propionate oxidation in wild-type and citrate synthase mutant *Escherichia coli:* evidence for multiple pathways of propionate utilization. *Biochem J*. 1993;291(Pt 3):927-932. doi:10.1042/BJ2910927.
44. Breidt F, Medina E, Wafa D, et al. Characterization of cucumber fermentation spoilage bacteria by enrichment culture and 16S rDNA cloning. *J Food Sci*. 2013;78(3):M470-M476. doi:10.1111/1750-3841.12057.
45. Koenig GL. Viability of and plasmid retention in frozen recombinant *Escherichia coli* over time: a ten-year prospective study. *Appl Environ Microbiol*. 2003;69(11):6605-6609. doi:10.1128/AEM.69.11.

Appendix

Abbreviations

ANOVA	Analysis of variance
AU	Arbitrary units
CFU	Colony-forming units
DMEM	Dulbecco's modified Eagle medium
FSC	Forward scatter
FSC-A	Forward scatter area
FSC-H	Forward scatter height
GC-MS	Gas chromatography–mass spectrometry
GFP	Green fluorescent protein
HPLC	High-performance liquid chromatography
IBS	Irritable bowel syndrome
IBS-C	Irritable bowel syndrome with constipation
IBS-D	Irritable bowel syndrome with diarrhea
IPTG	Isopropyl β-D-1-thiogalactopyranoside
LB	Luria–Bertani
MFI	Mean fluorescence intensity
OD600	Optical density at 600 nm
PBS	Phosphate-buffered saline
PFA	Paraformaldehyde
ROC	Receiver operating characteristic
rpm	Revolutions per minute
SSC	Side scatter
SSC-A	Side scatter area
SCFA	Short-chain fatty acid
SD	Standard deviation
SEM	Standard error of the mean.